BJRS

BRAZILIAN JOURNAL
OF
RADIATION SCIENCES
07-03 (2019) 01-21

Preclinical dosimetric evaluation of Ixolaris labeled with ^{99m}Tc and Translational Model

Soriano[a] S.C.S., Barboza[b] T., Souza[b] S.A.L., Sá[a] L.V.

[a] *Instituto de Radioproteção e Dosimetria (IRD)/Comissão Nacional de Energia Nuclear (CNEN), 22783-127, Rio de Janeiro, RJ*
[b] *Hospital Universitário Clementino Fraga Filho(HUCFF)/Universidade Federal do Rio de Janeiro, 21941-913, Rio de Janeiro, RJ*
sarahsoriano@bolsista.ird.gov.br

ABSTRACT

This study aimed to investigate ^{99m}Tc- Ixolaris uptake by body in mice by means of an scintigraphic imaging dosimetry method to estimate the absorbed and effective doses resulting from the diagnosis of melanoma and metastases in humans. C57BL6 mice induced animals with cell line B16-F10 murine melanoma were tested. It was determined by Single Photon Emission Tomography Computed (SPECT) images a latency period of 15 to 21 days for the development of lung metastasis in mice. The radiopharmaceutical was intravenously administered in a caudal vein, and SPECT images were acquired approximately at 0.5 h, 1.5 h, 2.5 h, 3.5 h and 24 h post-administration for analysis and quantification. The biokinetics model was determined and cumulative activity to estimate the absorbed dose in each organ was calculated. The mass and metabolic differences between mice and humans were considered and used to extrapolate the data for different scales. Absorbed doses in irradiated target organs were calculated for the source organs based on dose factors provided by the software MIRDOSE and Olinda/EXM. Afterwards, the effective doses were estimated. The metabolic differences were 7,02 in this study. The dosimetric results indicated an estimated effective dose of 4.3 mSv for diagnostic exams conducted in human melanoma patients for an administered activity of 25.7 MBq. Comparing with effective doses resulting from other ^{99m}Tc diagnostic techniques, effective dose ranging from 0.6 to 4.8 mSv it was concluded that the procedure should proceed into a Clinical Phase in humans.

Keywords: preclinical dosimetric, ^{99m}Tc- Ixolaris, SPECT, imaging dosimetry method.

ISSN: 2319-0612
Accepted: 2019-05-23

1. INTRODUCTION

The biodistribution study of tracers in animals is the first step in the development of any radiopharmaceutical that will be subsequently administered in humans. Animal models have been used to develop new drugs to human health, being a useful and effective practice to avoid adverse effects since the 1950s, after the thalidomide scandal when several babies were born with severe deformities in the lower and upper limbs extremities (1).

Over the past 15 years, there has been a great deal of progress in the development of methods for accurately quantifying nuclear medicine images (2). Imaging dosimetry becomes an important method because it is a personalized dose distribution analysis and it is non-interventionist. (3). Dose calculations based on this approach depend on high-quality SPECT (Single Photon Emission Computed Tomography) image quantification, which is generally more reliable than planar methods, but it is also more time and labour-intensive. If done well, however, with appropriate radiation transport methods, one obtains 3D estimates of radiation dose. This is a more sophisticated approach, as it is used in external beam radiotherapy and will eventually allow internal dose planning with radiopharmaceuticals to be employed in the same way (4).

The analysis of skin cancer has increased over time around the world. Malignant melanoma is less frequent than non-melanoma skin cancer, but is much more aggressive, with a high mortality rate. Early therapy may reduce the use of aggressive therapies such as chemotherapy and radiation therapy, and decrease the risk of developing metastases.

Barboza et al. (5) developed a new radiopharmaceutical, ^{99m}Tc-Ixolaris, based on a Tissue Factor inhibitor present at the salivary gland of the tick *Ixodes scapularis*. The images of this new radiopharmaceutical affinity in organs of interest for melanoma diagnosis in animals and the biodistribution and dosimetric study were performed. Thus, the development of a diagnostic tool increases the possibility of evaluation and follow-up of patients with melanoma, through the understanding of pathophysiological mechanisms.

This study aims to quantify the biodistribution of ^{99m}Tc-Ixolaris in C57BL6 mice, from CT and SPECT images since this is a promising tool in melanoma diagnosis. Through the biodistribution model in mice, this dosimetric study aims to provide data for the future use of this radiopharmaceutical in humans; however it is necessary to carry out the clinical study.

2. MATERIALS AND METHODS

The procedure applied to animals followed the patterns described for the use of experimental animals, approved by National Counsel of Animal Experimentation Control (CONCEA).

The murine melanoma cell line B16-F10 was induced by intravenous administration in two young male adults C57BL6 mice weighing between 25 and 30 g. In 16 to 17 days after induction, the labelling of Ixolaris, a 15,000 Dalton protein, with two *Kunitz*-like domains, with ^{99m}Tc was performed and the main quality control tests were executed: radiochemical purity, radionuclide purity, labelling stability and pH.

2.1. Radiopharmaceutical

In the direct labelling process of Ixolaris with 99mTc a concentration of 15 μg / mL of stimulating reducing agent (SnCl2 - Sigma Aldrich, USA) sterilized with a 0.22 μm Millipore® filter and 1 μg of Ixolaris was applied.

The test was performed under a pressure test, under a vacuum using the syringe, in laminar flow with autoclaved materials. The Ixolaris and SnCl2 were incubated for ten minutes at room temperature (21°C) and then 37 MBq (1 mCi) was added to the incubation for over ten minutes at room temperature (21°C), ending the marking process.

The determination of radionucleic purity can be performed by an energy tracing method, since the energy of ^{99}Mo (740 KeV) is much higher than that of ^{99m}Tc (140 KeV). Two measurements of

the same eluate were performed. First, the eluate was measured inside a 6 mm thick lead vial, which attenuates almost all of the ^{99m}Tc 140 keV gamma rays, with ^{99}Mo activity recorded. Subsequently, only the eluate was measured and ^{99m}Tc activity was recorded. Then, it was possible to calculate the amount of ^{99}Mo present and express it through the ratio ^{99}Mo / ^{99m}Tc [μCi / mCi].

Radiochemical purity (Equation 4) was determined by thin layer chromatography (TLC) using Whatmann No. 1 paper and acetone (ISOFAR®) as mobile phase, gel filtration liquid chromatography (Sephadex® G-75).

Chromatography on paper, a glass tube containing acetone (ISOFAR®) was used as the mobile phase, capped with a lid, to perform the ascent chromatography; and Whatman #1 paper strips are divided into 4 equal parts, to delimit the tape at the origin and top. An aliquot of the radiopharmaceutical was applied close to the 2 cm mark of origin to start the ascending chromatography (Barboza, 2103).

Upon arrival of the mobile phase in the line delimiting the top, the paper strips were withdrawn from the chromatography tubes and placed to dry at room temperature. With the dried strips, these were cut into 4 parts in order to identify the location of the labeled molecule along the tape. All pieces of the tapes were placed for radioactive counting on gamma counter (Wizard2, PerkinElmer®).

The stability of the labeling was determined by thin layer chromatography (TLC) using Whatmann No. 1 paper and acetone (ISOFAR) as mobile phase, gel filtration liquid chromatography (Sephadex® G-75). This test was evaluated by incubation in saline solution (0.9% NaCl2) and C57BL6 mouse plasma for different periods of time, following the labeling analysis immediately and at 1, 3, 5 and 24 hours (Barboza, 2013).

$$\%radiolabelling\ efficiency = \frac{(n°half-count\ of\ the\ lower\ or\ upper\ tape)}{total\ count} \text{ X } 100 \qquad \text{(Equation 1)}$$

The percentage of impurity was calculated considering the Rf (delay factor) of TcO_4^- and TcO_2:

$$\%\ TcO4- = \frac{(Radioactivity\ Rf\ 1{,}0)}{Total\ radioactivity} \qquad \text{(Equation 2)}$$

$$\%\,TcO2- = \frac{(Radioactivity\ Rf\ 0{,}0)}{Total\ radioactivity} \quad \text{(Equation 3)}$$

$$\%Rp = 100 - (\%TcO_4) - (\%TcO_2) \quad \text{(Equation 4)}$$

2.2. Image acquisition

An activity of 25 MBq of the ^{99m}Tc-Ixolaris was administered in mice and serial images of the induced (n=2) and control animal (n=1) were acquired were acquired approximately at 0.5 hour, 1.5 hours, 2.5 hours, 3.5 hours and 24 hours after intravenous injection.

For dosimetric studies, two SPECT cameras (*GE Millennium, Xeleris workstation)* were used. Each acquisition was performed for 20 minutes, 32 frames, matrix 128 x 128, and zoom of 4.00. The OSEM / MLEM iterative reconstruction method with 6 iterations and Butterworth filter 0.5 frequency cut applied, with up to 10 images for each group. SPECT quality control tests were performed during the period between administration and the first image.

2.3. Quantification by image

The quantification was performed within regions of interest (ROI) positioned in organs of interest for the time series described above. To anatomically identify the uptake in the organs, SPECT images were fused with CT images held on an Optima 560 PET/CT (GE Healthcare), located in the same hospital.

The number of mean counts and respective associated uncertainties within ROI selection was performed with OsiriX® software and were used for quantification. From the count values, the activities were obtained in time intervals using the volumetric sensitivity determined for ^{99m}Tc radionuclide. With this information, it was possible to obtain the accumulated activity (Equation 5), later corrected by the mass (Equation 6) and metabolic factors (Equation 7) of the difference

between animals and humans (6), because the smaller animals tend to have the fastest metabolism, so we can not admit that human dosimetric data are the same as the dosimetric data of the mice studied in this study. Therefore, there is a need for extrapolation data through an allometric scale.

$$\tilde{A}_{corrected} = \tilde{A} \cdot f_{mas} \cdot f_{met} \quad \text{(Equation 5)}$$

$$f_{mas} = \frac{\frac{m_{oh}}{m_{ch}}}{\frac{m_{oa}}{m_{ca}}} \quad \text{(Equation 6)}$$

Where,

f_{mas}**:** massic factor.

m_{oh}: human organ mass.

m_{ch}: human body mass.

m_{oa}: animal organ mass.

m_{ca}: animal body mass.

$$f_{met} = \left(\frac{m_{ch}}{m_{ca}}\right)^{1/4} \quad \text{(Equation 7)}$$

where,

f_{met}: metabolic factor.

Absorbed doses were calculated by MIRD Pamphlet 11 (7) and OLINDA EXM software to compare the results with the ones observed in other studies (8). Accumulated activities in each organ based on dose factors provided by the software MIRDOSE and Olinda (*S* factor) and absorbed doses in target organs were calculated. The effective doses were estimated through radiation weighting factors (w_R) and tissue or organ weighting factor (w_T) provided by ICRP 103 (9).

2.4. Uncertainty analysis

The activity meter uncertainty of 4.5% was determined from traceability and intercomparison with the National Metrology Laboratory of Ionizing Radiation (LNMRI) in Brazil. The uncertainty for the mice weight used in this study was 0.01%. The uncertainty associated with visual acuity during ROI delimitation was determined performing 10 different measures in the same region; it was noted a 10% variation between scores. Thus, the uncertainty attributed to the absorbed dose was 10% since other uncertainties were considered ten times lower compared to those associated with visual acuity.

3. RESULTS AND DISCUSSION

3.1. Radiopharmaceutical

The amount of ^{99}Mo present is expressed through the ratio ^{99}Mo / ^{99m}Tc [μCi / mCi]. The amounts of ^{99}Mo and ^{99m}Tc present in the eluate used for labeling the Ixolaris molecule are described in Table 1.

Table 1: Result of radiochemical purity test.

Background radiation (μCi)	***^{99}Mo reading (μCi)***	***^{99m}Tc reading (μCi)***	***^{99}Mo/^{99m}Tc (μCi/mCi)***	***Concentration ^{99m}Tc of elution (mCi/ml)***
2,57	1,66	545	0,001	90,9

The limits of the European and American Pharmacopoeias are respectively 0.1% and 0.15%, so the radiochemical purity of the eluate used was 0.1%, an adequate value in comparison to the references. It was concluded that the amount of ^{99}Mo present in the eluate did not compromise our experiment.

The determination of radiochemical impurities resulting from the radiolabelling process of ixolaris with Technetium-99m (^{99m}Tc) was done with three chromatographic techniques. The first technique used was paper chromatography (Whatman N° 1) with acetone as the mobile phase (n = 6). Under these conditions TcO_4^- in acetone has Rf = 1 and the labeled complex (^{99m}Tc-ixolaris) Rf = 0. Graph 1 demonstrates the labeling efficiency and the presence of TcO_4^- over time, and it is possible to notice the elevation of TcO_4^- only 24 hours after the labeling, at which point the radiopharmaceutical would no longer be used for in vivo administration. This turned possible the use of the radiopharmaceutical for up to 3 hours. In our experiments the radiopharmaceutical was used in the first hour. The second technique used was Sephadex G-75 gel filtration chromatography (n = 3), which separates the compounds by molecular weight. In this experiment it was demonstrated that the complex formed ^{99m}Tc-Ixolaris was blunt, and its elution was detected early when compared to $Na^{99m}TcO_4$, this data has been published in Barboza et al, 2015. The third and final technique for determination of radiochemical purity was thin layer chromatography using silica gel coated fiber sheets (TLC-SG) (n = 6) (table 2), using acetone and 85% methanol as the solvent for determination of the amount of TcO_4^- and TcO^2, respectively. Through this method the radiochemical purity of the ^{99m}Tc-ixolaris was higher than 90% in all the periods (0, 1, 3, 5 and 24h) evaluated.

The larger presence of TcO_4^- (2.6 ± 0.53) was observed 24h, as well as the larger presence of TcO_2 (5.13 ± 0.72). These data can also be confirmed through the images presented in this article, because another organ of importance for assessing the excessive presence of TcO_2, the spleen, no increased uptake is observed in both the experimental and control animals. The presence of colloids formed by the complex ^{99m}Tc-ixolaris from the first hours is low, being implied from the normal biodistribution of this radiopharmaceutical its presence in the liver; and in the lungs when metastasized, due to its ability to bind to the tissue factor expressed in tumor cells.

Figure 1: *^{99m}Tc-Ixolaris complex ascending Chromatography in Whatman paper No 1. Result express mean SD (n = 6).*

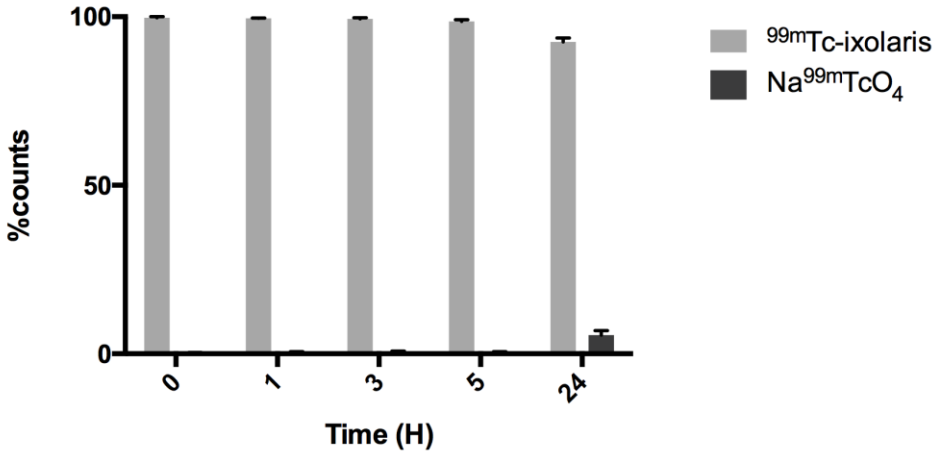

The table 2 demonstrates the products generated after radiolabeling using $SnCl_2$ as by-products of this process. The presence of both TcO_4^- and TcO_2 up to 3 h is low and does not compromise the quality of the data found and is not solely responsible for the uptake observed in the liver and lungs. The concentration of both by-products is high in 24 hours when the radiopharmaceutical will no longer used. The observed radiochemical purity (% Rp) remained above 90% in all observed periods, with the radiopharmaceutical administered within one hour after its production for the experiments performed.

Table 2: Results of chromatography

		Time (h)									
		0		***1***		***3***		***5***		***24***	
		MD	***SD***	***MD***	***SD***	***MD***	***SD***	***MD***	***SD***	***MD***	***SD***
TLC-SG	***% TcO_4-***	0.09	0.05	0.15	0.17	0.24	0.12	0.35	0.2	2.6	0.53
	% TcO_2	0.13	0.08	0.23	0.11	0.18	0.13	0.39	0.09	5.13	0.72
	%Rp	99.78	0.1	99.65	0.1	99.57	0.14	99.27	0.15	92.27	0.47

The pH of this solution was 7.0, ie, neutral pH. The ideal blood pH is in the range of 7.36 to 7.4. If too acidic or basic solution is given to the patient, it can cause coma and seizure, respectively. Therefore, pH equal to 7 of ^{99m}Tc - Ixolaris is the ideal to be administered to the patient.

3.2. Quantification by image

The three analysed animals were anesthetized and weighed, and the administration of the radiopharmaceutical was performed.

For each animal, five SPECT images related to five different times were acquired to analyse the source organs. The figures 1, 2 and 3 illustrate the images from the animals tested.

Figure 2: *SPECT images of the CONTROL animal (29,47 g) for 1.58 h, 3.45 h, 4.40 h, 5.63 h, and 24.26 h after radiopharmaceutical administration (23,14 MBq).*

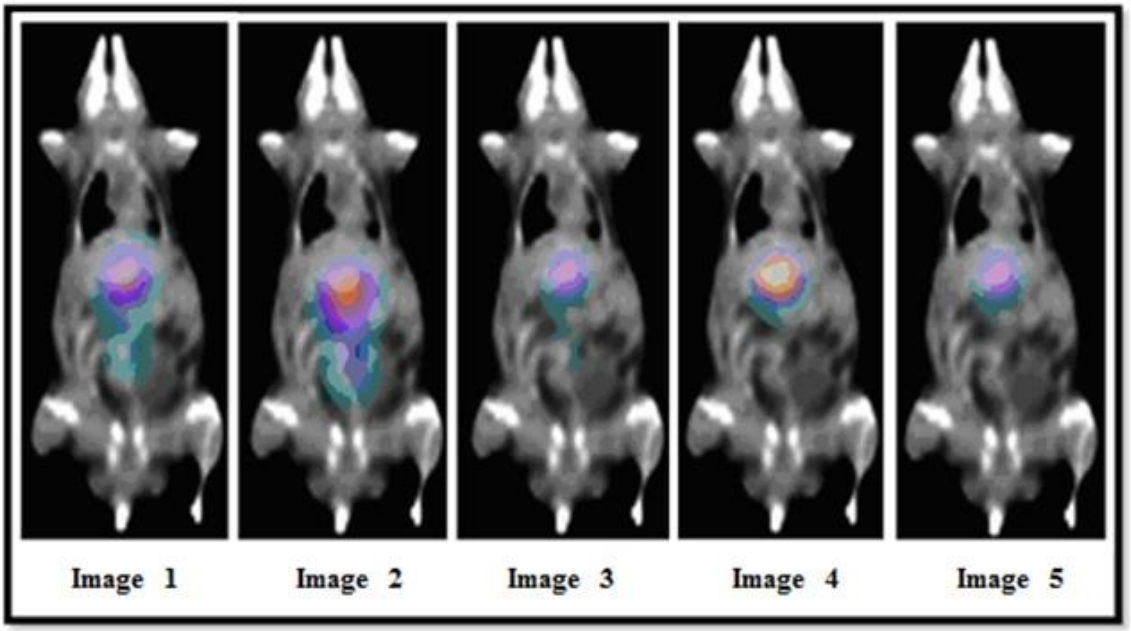

Figure 2 shows that the uptake organs for the CONTROL animal (healthy) were the liver and the bladder. The uptake in the bladder from image 2 is higher than in Image 1, meaning that the

maximum uptake occurs between 1.5 h and 3.5 h. In Image 3, a subsequent decrease in liver uptake can be seen, and the images 4 and 5 show biological excretion associated with physical decay.

Figure 3: *SPECT images of the INDUCED A animal (28,60 g) for 0.68 h, 1.85 h, 2.70 h, 3.70 h and 24.71 h after radiopharmaceutical administration (25,12 MBq).*

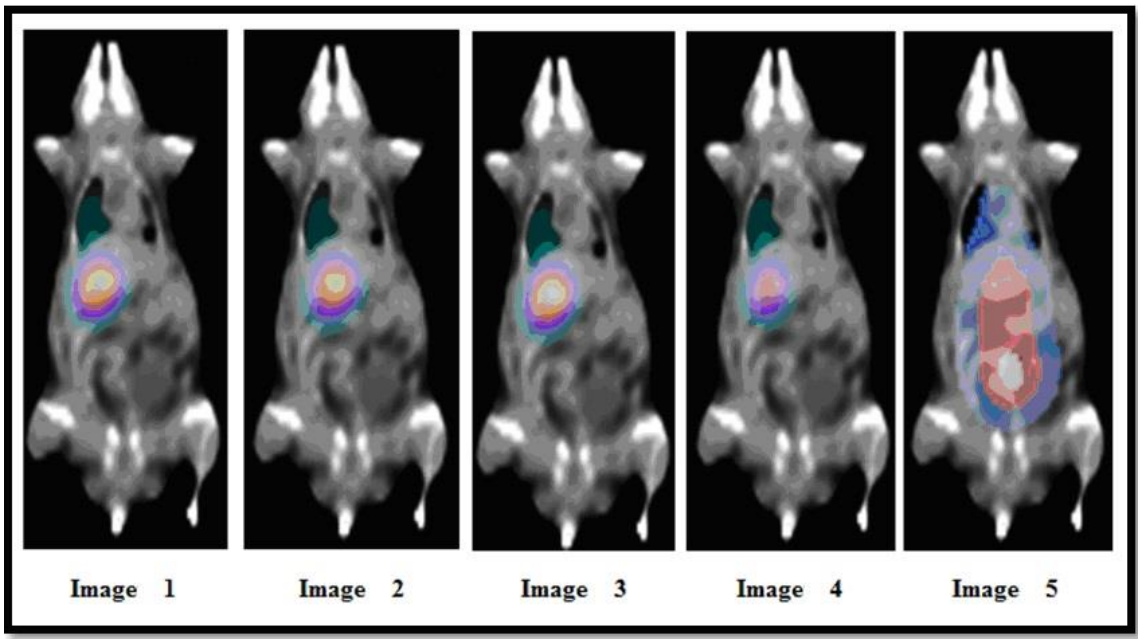

Figure 3 shows the images for the INDUCED A animal where uptake in the liver, lung and bladder can be observed. Analysing images 1, 2, 3 and 4, there is a progressive decrease in the radiation intensity, indicating physical decay. In Image 5, there is still liver and lung uptake, and also in the bladder, indicating urinary excretion.

Figure 4: *SPECT images of the INDUCED B animal (27,65 g) for 0.55 h, 1.60 h, 2.61 h, 3.50 h and 23.63 h after radiopharmaceutical administration (26,29 MBq).*

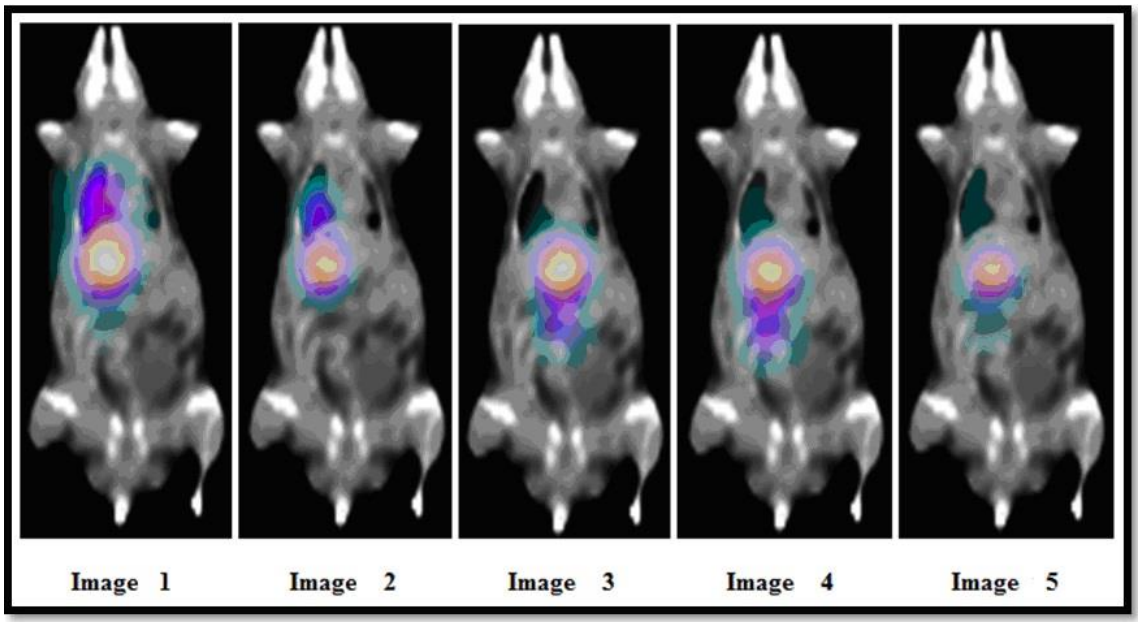

Figure 4 shows the images for the INDUCED B animal in which there are only liver and lung uptakes. It can be noted the progressive decrease of uptake in the left lung and liver, concomitantly with the increase of uptake in the bladder, again demonstrating the excretion and physical decay.

It was observed that the uptake of ^{99m}Tc-Ixolaris in healthy animals occurred in the liver and bladder, while in animals with melanoma it was in the liver, bladder and left lung.

From the activity *versus* time curve of the CONTROL animal, Figure 5, it can be observed that the liver uptake is approximately 1.6 times greater than bladder elimination and, the liver curve follows the theoretical pattern associated with the biological elimination and physical decay. The bladder curve shows the moment of maximum uptake in second point. Later, the physical and biological decay can be seen.

Figure 5: *Activity versus time curve of uptake organs (liver and bladder) of the CONTROL animal*.

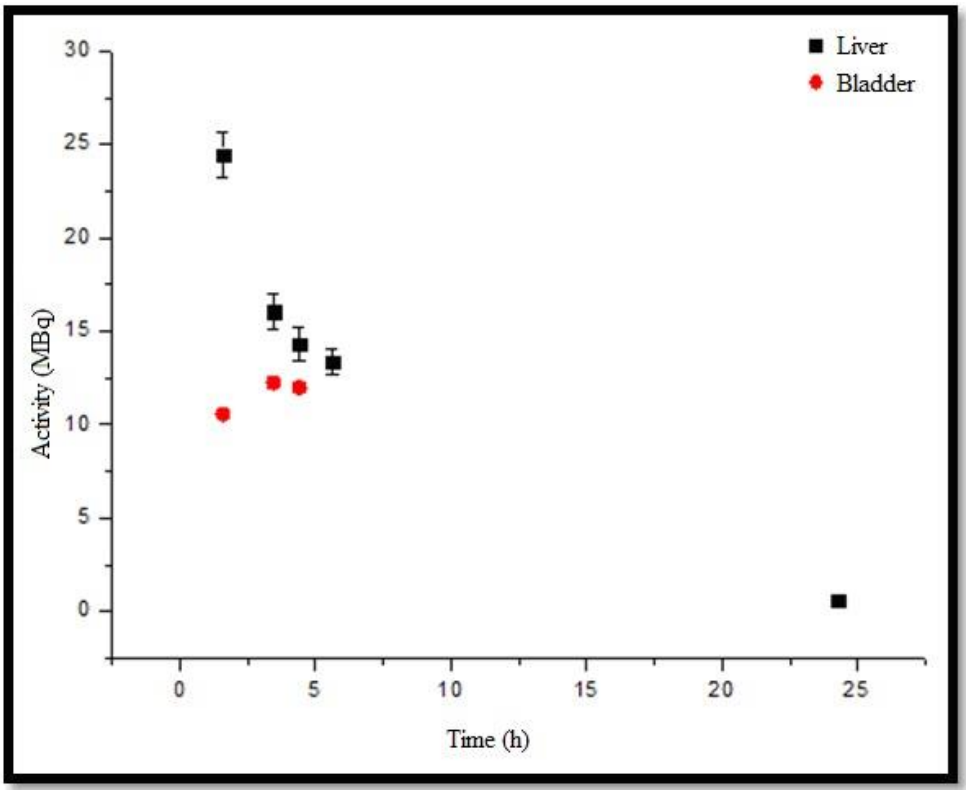

Figure 6 shows the activity *versus* time curves for INDUCED A animal showing the uptake of target organs, emphasizing that the liver uptake is approximately 2.9 times greater than the lung elimination. The liver and the left lung demonstrated similarity with the physical decay curve.

Figure 6: *Uptake organ activity versus time curve (liver, lung and bladder) of INDUCED A animal*

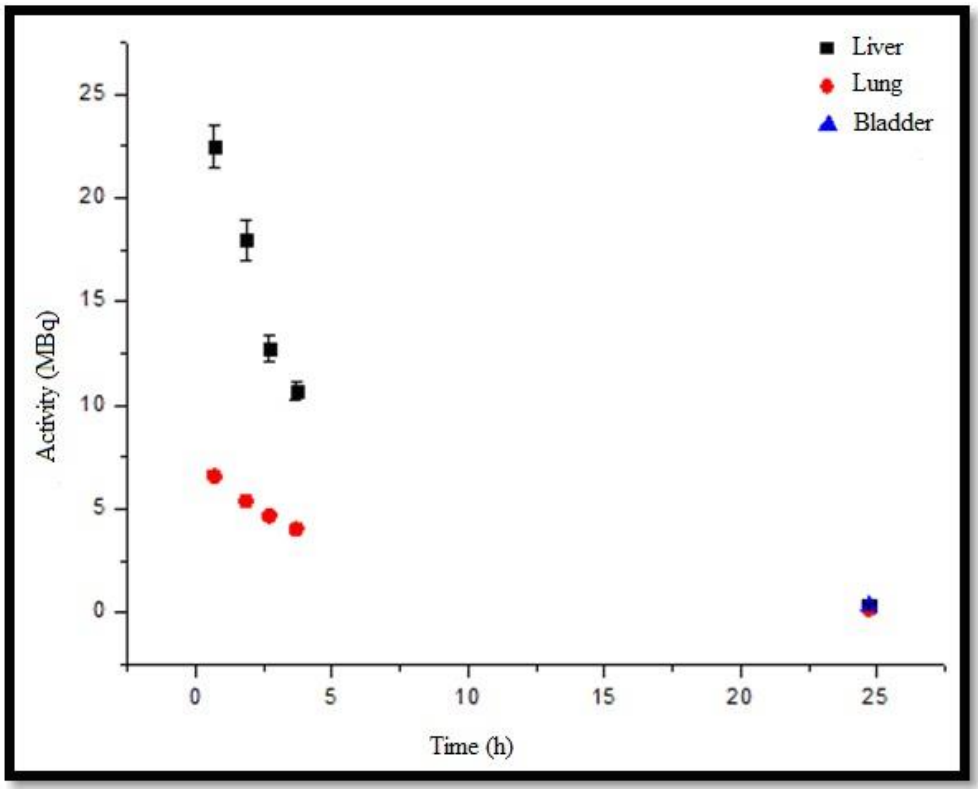

For INDUCED B animal, Figure 7, it can be observed that the liver uptake is approximately 3.8 times greater than the lung uptake and 1.4 times greater than the elimination by urinary bladder. It can be also seen that the liver curve follows the theoretical pattern combining the biological elimination and physical decay. The lung curve shows the time of maximum uptake between the first and the third point; later it can be seen the physical and biological decay.

Figure 7: *Uptake organs activity versus time curve (liver, lung and bladder) for INDUCED B animal*

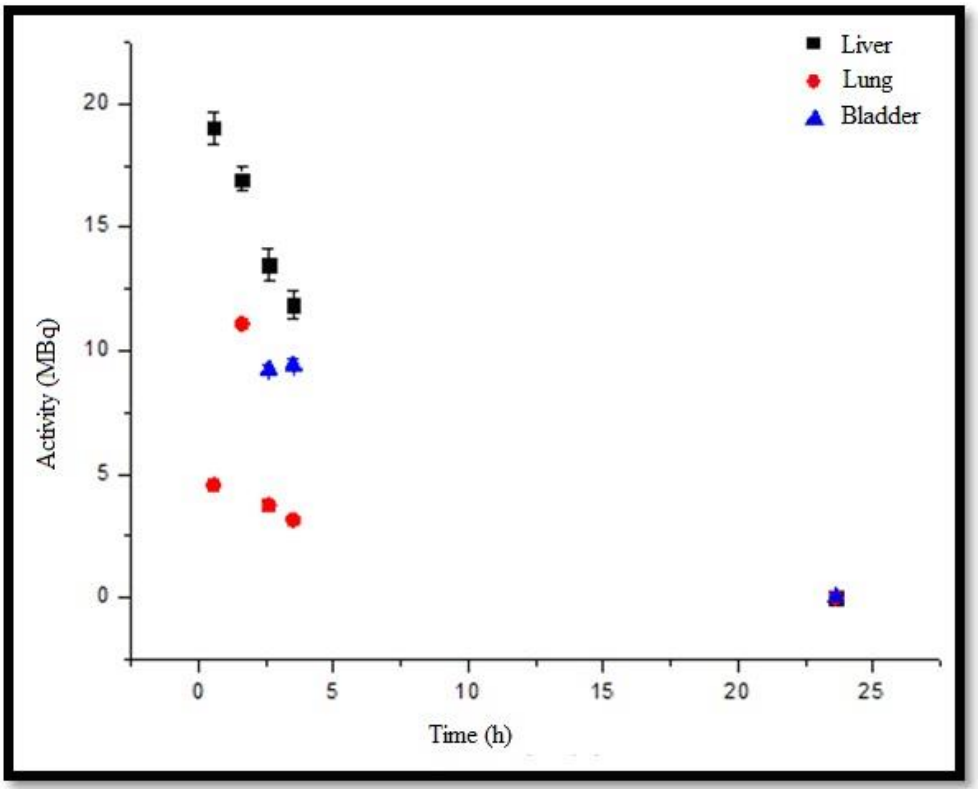

Because there is no published reference organ mass for mice, the average of animal organ mass used in this work was considered and are presented in Table 3.

Table 3: Humans and mice standard masses [b](10).

Organ	***Standard Mass (g)***	
	Human [b]	***Mice***
Whole Body	73000	30.00
Liver	1800	1.45
Lung	1200	0.32
Bladder	200	0.05

In this work was used the metabolic factor of 7.02, in addition to mass flow factors frequently used for imaging dosimetric calculations. The mass factors applied were 0.51 for liver, lung and 1.51 to 1.64 for the bladder, which carry a metabolic mass and a correction factor of 3.58 for the liver, 10.60 for lung and 11.51 to the bladder.

The results obtained of accumulated activities (Ã) which represents an integral time of curvature, that is, an area under the curve, are shown in Table 4. Thus, obtaining the total of disintegrations that occur over time in a region of interest in animal. The accumulated activities corrected ($Ã_{corrected}$) is the same information, but in human estimate from the animal.

The residences times (τ), for each human organ estimated from each animal are shown in Table 4.

Table 4: Accumulated activities (Ã), accumulated activities corrected ($Ã_{corrected}$) and residence time (τ) for each human organ estimated from – CONTROL and INDUCED (animal A and animal B).

Animal	***Parameter***	***Lung***	***Liver***	***Bladder***
CONTROL	**Ã (MBq.h)**	-	198.91	32.81
	$Ã_{corrected}$ (MBq.h)	-	712.09	377.64
	τ (h)	-	30.77	16.31
INDUCED A	**Ã (MBq.h)**	59.60	164.28	0.32
	$Ã_{corrected}$ (MBq.h)	631.76	588.12	3.68
	τ (h)	25.15	23.41	0.15
INDUCED B	**Ã (MBq.h)**	50.36	164.86	102.99
	$Ã_{corrected}$ (MBq.h)	533.82	590.19	1185.41
	τ (h)	20.30	22.45	45.08

It can be seen that the organs that had higher residence times were the liver and lung, in ascending order, and sometimes the bladder. So, these organs have higher total number of disintegrations that occurred for a given integration time per unit of activity initially administered.

The differences observed in INDUCED data, among the accumulated activity values, corrected cumulative activity and residence time for the bladder are due to the different acquisition times for the images whether urinary excretion occurred or not, with no possibility of control during the experiment.

Absorbed doses in the target organs due to source organs (liver, lung and bladder) in humans were calculated from the *S factors* for ^{99m}Tc by the MIRD Pamphlet 11 publication and Olinda EXM software, which are shown in Table 5.

The results for the two methods are very similar for all organs, while some *S factors* are set often complementary in each method. Thus, by using both, it was possible to estimate the absorbed dose to a larger number of organs studied.

As the comparison between different procedures and even risk estimation are carried out through effective dose values, these were calculated using the radiation weighting factor (w_R) for photon and tissue weighting factors (w_T), both established in (9).

According to the absorbed doses calculated from the *S factors* provided by the software MIRDOSE, the effective dose observed in the human body for the developed ^{99m}Tc – Ixolaris radiopharmaceutical was (4.07 ± 0.45) mSv; for data obtained by OLINDA software the effective dose in human body was (4.49 ± 0.49) mSv.

It is known that for medical exposures there is no dose limitation. However, reference levels, i.e. guideline levels, are used in medical imaging to indicate whether under routine conditions the dose for the patient or the amount of radiopharmaceutical administered in a specific examination is abnormally high or too low for the procedure.

For ^{99m}Tc – Ixolaris radiopharmaceutical development, the obtained effective doses were compared to the effective doses normally used for routine tests with the same ^{99m}Tc radionuclide, as show in table 6.

Table 5*:* Absorbed doses in the target organs due to source organs (liver, lung and bladder) in humans using the *S factors* from MIRDOSE and OLINDA references.

Target organ	***Absorbed dose (mGy)***	
	MIRD	***OLINDA***
Spleen	0.61 ± 0.07	0.52 ± 0.06
Osteogenic Cell	-	0.84 ± 0.09
Brain	-	0.02 ± 0.00
Liver	7.75 ± 0.85	7.14 ± 0.78
Small Intestine	0.77 ± 0.08	0.75 ± 0.08
Breast	-	0.64 ± 0.07
Red Marrow	0.91 ± 0.10	0.58 ± 0.06
Muscle	-	0.63 ± 0.07
Ovary	1.26 ± 0.14	1.25 ± 0.14
Pancreas	1.12 ± 0.12	1.21 ± 0.13
Bladder Wall	25.74 ± 2.83	23.57 ± 2.59
Gallbladder Wall	-	2.08 ± 0.23
Heart Wall	-	1.42 ± 0.16
Stomach Wall	0.63 ± 0.07	0.61 ± 0.07
Lower Large Intestine Wall	1.24 ± 0.14	1.27 ± 0.14
Upper Large Intestine Wall	0.79 ± 0.09	0.78 ± 0.08
Skin	0.25 ± 0.03	0.24 ± 0.03
Lung	8.59 ± 0.94	7.94 ± 0.87
Kidneys	0.80 ± 0.09	0.80 ± 0.09
Adrenals	1.17 ± 0.13	1.43 ± 0.16
Bone Surface	0.56 ± 0.06	-
Testicles	0.77 ± 0.08	0.80 ± 0.09
Thymus	-	0.73 ± 0.08
Thyroid	0.17 ± 0.02	0.20 ± 0.02
Uterus	2.65 ± 0.29	2.73 ± 0.30

Table 6: Effective doses for diagnostic exams with radiopharmaceuticals (11).

Exam	***Radiopharmaceutical***	***Level Reference (MBq)***	***Effective Dose (mSv)***
Brain Flow	^{99m}Tc-HMPAO	500	5.5
Bone Scan	^{99m}Tc-Fosfato	600	4.8
Myocardial	^{99m}Tc-Isonitrilas	600	4.2
Bone Scan	^{99m}Tc-MDP	500	3.6
Brain Scan	^{99m}Tc-Pertecnetato	500	2.7
Thyroid Image	^{99m}Tc-Pertecnetato	200	2.6
Kidneys	^{99m}Tc-DMSA	160	2.5
Kidneys	^{99m}Tc-DTPA	350	2.2
Lung Perfusion	^{99m}Tc-MAA	100	1.2
Lung Ventilation	^{99m}Tc-Aerossol	80	0.6
Liver and Spleen	^{99m}Tc-Coloide	80	0.6

The dosimetric study of the radiopharmaceutical ^{99m}Tc-ixolaris of C57BL6 mice induced with the murine melanoma B16-F10 cells was carried out in order to determine their biokinetic model. To obtain the absorbed doses resulting from the use of the new radiopharmaceutical, a dosimetry method of imaging and the translation method of mice to humans were used, considering the mass and metabolic differences between the two species.

From the images the biodistribution in the healthy animal was observed in the liver, with residence time of 30.77 h, and in the bladder, with a residence time of 16.31 h. For animals with induced melanoma, the biodistribution was observed in the liver (residence time averaged 22.93 h, lung (residence time averaged 22.73 h) and bladder (residence time ranging between 0.15 and 45.08 h). Given the residence times in human organs extrapolated from the information acquired in mice, it was concluded that the organs which had a higher total number of disintegrations (for a given integration time for initially given unit of activity) were the liver, lungs and, sometimes, the

bladder. Consequently, the organs that received higher absorbed doses were the liver (7.45 ± 0.74 mGy), lungs (8.26 ± 0.83 mGy), bladder (24.65 ± 2.46 mGy) and the target organ, uterus (2.69 ± 0.27 mGy).

It is worth noticing the importance of considering the mass differences between mice and humans as well as the metabolic differences, since it leads to a large increase in the estimated dose. Not considering these differences is the same as ensuring that, despite having different organs sizes in the body, rats and humans have the same metabolic rate, which is not true. In this work, from the man reference data provided by the ICRP 89 and from the data of mice experimentally calculated, we used the metabolic factor of 7.02, in addition to mass flow factors frequently used for imaging dosimetric calculations. The mass factors applied were 0.51 for liver, lung and 1.51 to 1.64 for the bladder, which carry a metabolic mass and a correction factor of 3.58 for the liver, 10.60 for lung and 11.51 to the bladder.

Absorbed doses in radiosensitive organs such as bone marrow and kidney were, respectively, 0.91 ± 0.10 mGy and 1.17 ± 0.13 mGy, suggesting that this radiopharmaceutical is safe.

Therefore, for humans with melanoma in which ^{99m}Tc-Ixolaris could be administered, the estimated effective dose would be 4.3 ± 0.5 mSv, value similar to other diagnostic techniques with the same radionuclide, ranging from 0.6 mSv to 4.8 mSv.

4. CONCLUSION

It can be concluded that the beginning of a clinical phase with human trials is safe, since both the estimated absorbed dose in critical organs and the effective doses were in agreement to the ones observed nowadays in other well-established methods.

ACKNOWLEDGMENT

This work was supported by the Nuclear Energy National Commission (CNEN), which provided a scholarship.

REFERENCES

[1] Martic-Kehl, R. Mschibli, A.P. Schubiger. Can animal data predict human outcome? Problems and pitfalls of translational animal research. **Eur J Nucl Med Mol Imaging**. 2012; 39:1492-1496.

[2] International Atomic Energy Agency – **IAEA. Human Health Reports No. 9 Quantitative Nuclear Medicine Imaging: Concepts, Requirements and Methods**. Vienne, 2014.

[3] G. Sgouros et al. Three-dimensional imaging- based radiobiological dosimetry. **Semin Nucl Med**. 2008. 38(5):321-334.

[4] M.G Stabin. **Fundamentals of Nuclear Medicine Dosimetry**. 1st ed. Nashville, TN, USA: Springer;2008.

[5] Barboza, T., Gomes, T., Mizurini, D., et. al. ^{99m}Tc-ixolaris targets glioblastoma-associated tissue factor: In vitro and pre-clinical applications. **Thromb Res** 2015,15:S0049.

[6] McParland, B.J. **Nuclear Medicine Radiation Dosimetry - Advanced Theoretical Principles**. 1st ed. Springer;2010.

[7] S, Absorbed Dose per Unit Cumulated Activity for Selected Radionuclides and Organs. MIRD Pamphlet #11 (**Society of Nuclear Medicine** 1975).

[8] Elvas, Vangestel, C., Rapic, S. Characterization of 99mTc- Duramycin as a SPECT Imaging Agent for Early Assessment of Tumor Apoptosis. **Mol Imaging Biol** 2015.

[9] International Comission on Radiological Protection – ICRP. Recommendations of the International Commission on Radiological Protection. **ICRP Publication 103** (2007).

[10] International Comission on Radiological Protection – ICRP. Basic Anatomical and Physiological Data for Use in Radiological Protection Reference Values. **ICRP Publication 89** (2002).

[11] International Atomic Energy Agency – IAEA. **Basic Safety Standards for Protection against Ionizing Radiation and for Safety of Radiation Sources**. Vien